ACS Synthetic Biology

Research Article

pubs.acs.org/synthbio

# Catch and Release: Engineered Allosterically Regulated β-Roll Peptides Enable On/Off Biomolecular Recognition

Beyza Bulutoglu, Kevin Dooley,[†] Géza Szilvay,[‡] Mark Blenner,[§] and Scott Banta*

Department of Chemical Engineering, Columbia University, New York, New York 10027, United States

Supporting Information

**ABSTRACT:** Alternative scaffolds for biomolecular recognition are being developed to overcome some of the limitations associated with immunoglobulin domains. The repeat-in-toxin (RTX) domain is a repeat protein sequence that reversibly adopts the β-roll secondary structure motif specifically upon calcium binding. This conformational change was exploited for controlled biomolecular recognition. Using ribosome display, an RTX peptide library was selected to identify binders to a model protein, lysozyme, exclusively in the folded state of the peptide. Several mutants were identified with low micromolar dissociation constants. After concatenation of the mutants, a 500-fold increase in the overall affinity for lysozyme was achieved leading to a peptide with an apparent dissociation constant of 65 nM. This mutant was immobilized for affinity chromatography experiments, and the on/off nature of the molecular recognition was demonstrated as the target is captured from a mixture in the presence of calcium and is released in the absence of calcium as the RTX peptides lose their β-roll structure. This work presents the design of a new stimulus-responsive scaffold that can be used for environmentally responsive specific molecular recognition and self-assembly.

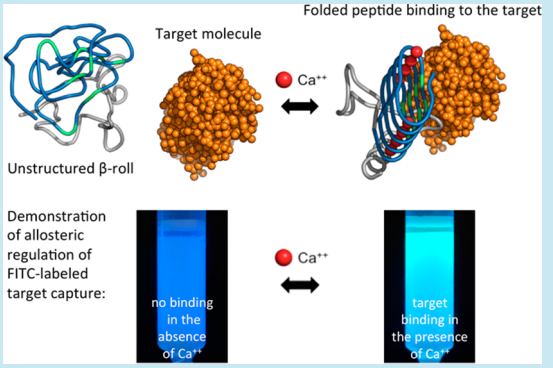


**KEYWORDS:** *disordered-to-ordered transition, protein switch, molecular recognition, RTX domain, conditional target binding*

Evolved biomolecular recognition is central for the continuity of life. Most regulatory and signaling events within and between cells depend on transient interactions between biomolecules. Antibodies have been the focus of the majority of biotechnology research involving biomolecular recognition and a great deal of effort has been focused on these immunoglobulin domains as engineered molecular recognition scaffolds.[1−3] Directed evolution techniques have enabled the development of molecular recognition scaffolds with features that can rival the performance of antibodies. Over the last few decades, alternative nonimmunoglobulin domains have been proposed for use in biomolecular recognition applications.[4−6] Affibodies, designed ankyrin repeat proteins (DARPins) and leucine rich repeats (LLRs) are among these alternative domains.[7−10]

There is also a great interest in conformationally dynamic systems, *e.g.*, protein switches, which allow for new control mechanisms over protein functions.[11−13] In nature there is a growing number of examples of proteins and peptides exhibiting conformationally dynamic behavior, which allows them to expand their biomolecular recognition capabilities.[14] This is exemplified by intrinsically disordered proteins, which have high-specificity and low-affinity interactions with multiple ligands.[15,16] For example, the C-terminal tail of the transcription factor p53 adopts different structures upon interaction with different partners, such that its dynamic conformation leads to multiple modes of binding.[15,17]

In this work, these concepts were combined and demonstrated *via* the selection of biomolecular recognition functionality in an allosterically regulated peptide scaffold: the Block V RTX domain of the adenylate cyclase protein from *Bordetella pertussis*. This peptide is likely unstructured in the absence of calcium ions and folds into the β-roll structure upon calcium binding. The β-roll secondary structure motif is a flattened corkscrew-like structure with β-strands separated by calcium binding turns that form two β-sheet faces each of which has 8 amino acids with solvent exposed side chains (Figure 1).[18−20] It has a repetitive sequence rich in glycine and aspartic acid, which are responsible for providing flexibility in the turns and for calcium binding.[20−24] It remains unfolded in low intracellular calcium concentrations (<0.1 mM) and when the adenylate cyclase protein is secreted C-terminus first, the RTX domain undergoes a polarized conformational change upon exposure to high extracellular calcium concentrations.[18,22,24,25] Thus, the β-roll structure serves as a calcium dependent switch to ensure the functional folding of the catalytic domain of the enzyme.[20,21] The folding of the isolated Block V peptide is reversible, calcium specific, requires C-terminal capping and is entropically stabilized.[23,26,27] Its native state with its polarized folding mechanism makes it a unique scaffold for exploring conditionally dependent biomolecular recognition. The re-

**Received:** March 22, 2017
**Published:** May 18, 2017

ACS Publications © XXXX American Chemical Society



DOI: 10.1021/acssynbio.7b00089
ACS Synth. Biol. XXXX, XXX, XXX−XXX

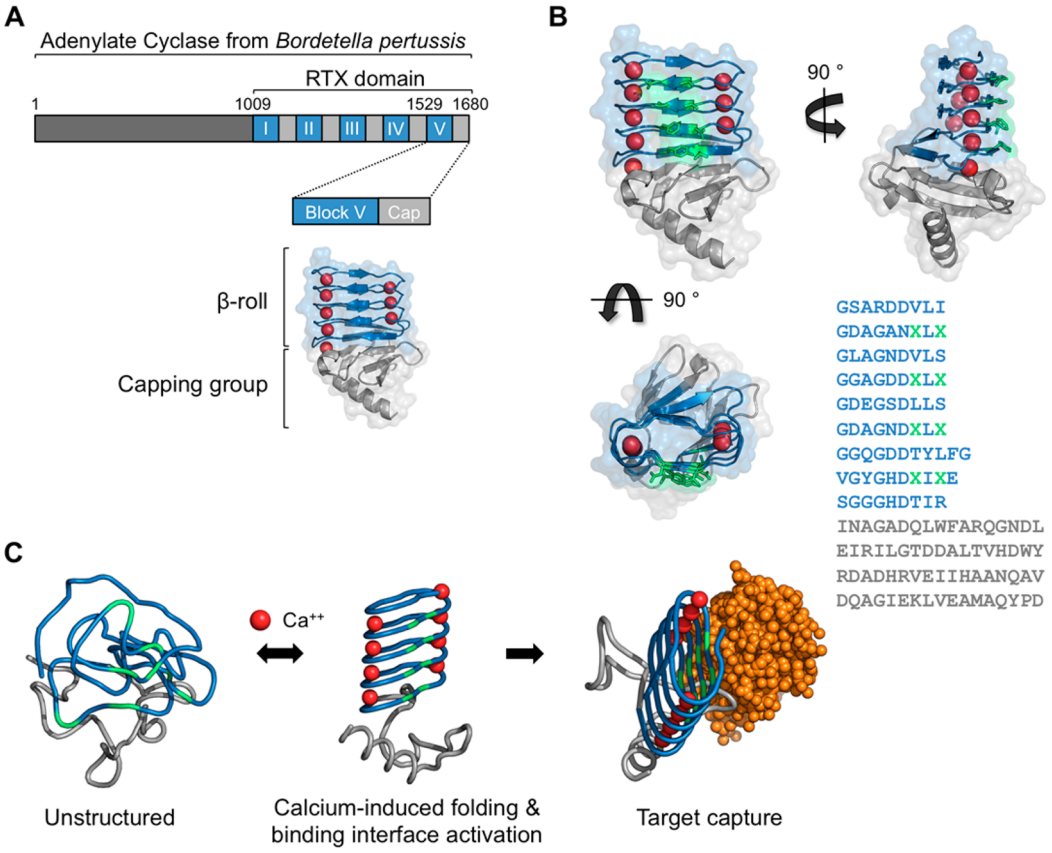


**Figure 1.** Structure of the $\beta$-roll peptide. (A) The adenylate cyclase enzyme has five RTX domains. The $\beta$-roll (blue) and its capping group (gray) are located between residues 1529 and 1680. The bound calcium ions are shown in red. (B) Protein structure and primary sequence. Eight residues of the $\beta$-roll face are highlighted in green. These positions (shown as X's in the protein sequence) were randomized in the created library. All figures were rendered in PyMOL using PDB file 5CVW.[22] (C) A cartoon demonstrating the switch mechanism of the peptide. It transitions from its unstructured state to the $\beta$-roll structure upon $Ca^{2+}$ binding. $Ca^{2+}$-triggered folding results in the formation of the binding interface (green) resulting in target (orange) capture.

cently discovered crystal structure of this domain has further elucidated its folding mechanism.[22]

This RTX domain exhibits disordered-to-ordered transition but it is not known to participate in biomolecular recognition. We hypothesized that amino acids on the $\beta$-sheet face of the folded $\beta$-roll domain could be engineered to create a binding interface, specifically controlled by the presence of calcium. A library of RTX mutants was created and several rounds of ribosome display were performed to select RTX mutants that conditionally bind hen egg white lysozyme, which has been a model target in directed evolution research.[28−30] By selecting peptides that bind the lysozyme target, we have begun to explore the idea of controllable assembly for conformationally dependent ligand capture. The reversibility of calcium binding allows the engineered molecular recognition to be controllable and thus, calcium-triggered target "catch and release" can be achieved.

## RESULTS AND DISCUSSION

**Mutation Positions and Library Generation.** The RTX domains of the adenylate cyclase protein from *Bordetella pertussis* and the location of the Block V domain are shown in Figure 1A. An advantage of using repeat scaffolds for molecular recognition is that the binding interface can be localized to a few amino acids in the repetitive sequence on the scaffold, making it easier to construct randomized libraries with defined surfaces for molecular recognition. In nature, the LLR repeat scaffold is used instead of immunoglobulin domains in the adaptive immune systems of some jawless vertebrates (*e.g.*, hagfish and lampreys).[31] We have identified two of the nine amino acids in the canonical $\beta$-roll peptide sequence that are not involved in turn formation, calcium binding, or creation of the hydrophobic core (Figure 1B).[22,23,25] These two amino acids are highly variable in all RTX domains, and are generally solvent exposed.[22,25,32] This creates an opportunity to vary these amino acids for desired new functionalities without compromising the unique and specific environmentally responsive behavior of the scaffold. These side chains were genetically randomized to create a library of new binding interfaces available to interact with target molecules when the peptide is in the folded conformation (Figure 1C). This allowed all mutants to retain the ability to adopt the $\beta$-roll structure in the presence of calcium, decoupling the amino acids involved in structure formation from those involved in molecular recognition. The degenerate NNK codon was used at the 8 positions to produce a library size of $20^8$ possible mutant Block V peptides.

**Library Selection Using Ribosome Display.** Selection techniques are critical for combinatorial protein engineering processes. Previously, we explored bacterial cell surface display and monovalent phage display as methods to form a genotype-phenotype linkage. However, these techniques proved to be difficult to use with the repetitive RTX domains. After several rounds of selection, frameshifts and stop codons within the $\beta$-


DOI: 10.1021/acssynbio.7b00089
ACS Synth. Biol. XXXX, XXX, XXX−XXX

roll sequences frequently accumulated. Ribosome display is not limited by the bacterial cell transformation efficiency and eliminates issues with clonal selection, where expression of truncated proteins is less taxing on cellular fitness than full-length mutants. Thus, this method was used and found to be more robust, enabling the reproducible selection of full-length sequences from the RTX peptide library (Figure S1). The capped RTX Block V library was subcloned into the pRDV vector for selection *via* this method.[9] Exclusion of a stop codon in the library transcripts allowed for the generation of ternary complexes composed of ribosomal subunits, mRNA, and the cognate translated protein, thereby maintaining a genotype-phenotype linkage (Figure S1). These complexes were used to select for clones that exhibited affinity toward immobilized biotinylated-lysozyme. Selections were performed in the presence of calcium to enable folding of the RTX domain. Consecutive rounds of biopanning in the presence of 10 mM calcium were performed starting with a subset of the library. A sample size of $1.1 \times 10^{12}$ transcripts were screened which corresponds to the expected library size. Screening of $3.3 \times 10^{12}$ sequences would be necessary ensure 95% screening coverage of the complete naïve library,[33] which suggests the library was not fully sampled. After six rounds of positive selections, the selected library converged to the sequence of P101 (Table S1).

In order to further explore the library, the procedure was repeated with iterative positive/negative selections. Following two rounds of biopanning in 10 mM calcium, the library was subjected to negative selection in 10 mM magnesium, which does not induce $\beta$-roll formation in the native sequence. Unlike with the positive selections, this approach did not converge to a dominant sequence and 10 mutants out of 34 sequenced full-length RTX variants were chosen for further evaluation (Table S2). Mutants with proline residues were assumed to be detrimental to the conformational change of the peptide and were avoided.[23,34] Priority was given to mutants rich in charged and hydrophobic residues, which frequently occupied mutated positions throughout the selected library (Table S3). The fact that the library did not converge with the positive/negative selections was surprising. Additional stringency could be incorporated in future experiments by using increased detergent concentrations or by extended off-rate selections.

**Determination of Binding Parameters *via* Isothermal Titration Calorimetry (ITC).** The interactions of the wild-type and mutant peptides (Figure S2A) with lysozyme were quantified using ITC. Unexpectedly, the wild-type peptide exhibited some affinity for lysozyme (dissociation constant ($K_d$) of 33 $\mu$M). After ITC analysis of 10 candidates, 3 mutants from the positive/negative selections were identified with improved affinities: PN206, PN406 and PN715, and the dissociation constants of these three mutants were similar to the P101 mutant from the positive selection (Table 1). The mutants demonstrated affinities that were an order of magnitude better compared to the wild-type peptide and the amino acids on the $\beta$-roll faces were mostly hydrophobic (Tables S1, S3).

The number of binding sites determined by fitting the ITC data varied between 0.45 and 0.85 (where 0.5 would indicate 2 RTX domains per one lysozyme molecule). The variation in these numbers could be due to nonspecific binding by some of the $\beta$-roll faces and further studies would be required to verify these interactions.

The mutant with the highest affinity, PN406 from the positive/negative selections, was found to bind lysozyme with a $K_d$ of 2.3 $\mu$M. It is interesting that the positive selection led to a single dominant sequence while the positive/negative selections did not converge and yet the affinities of the chosen mutants were similar to the mutant from the positive selection library. It is possible that positive/negative selections did not converge because there are several mutants in the library with similar affinities, which were possibly being coselected simultaneously. The fact that the positive/negative selections retained mutants with wild type affinity suggests the selection was less stringent than the positive selections alone. One explanation could be related to potential nonspecific interactions with lysozyme.

**Table 1. Binding Parameters of Wild-Type and Mutant Peptides**[a]

| peptide | dissociation constants ($K_d$, $\mu$M) | number of binding sites ($N$) |
|---|---|---|
| WT | 33 ± 10 | 0.46 ± 0.10 |
| P101 | 3.2 ± 0.7* | 0.55 ± 0.09 |
| PN206 | 6.2 ± 2.5* | 0.49 ± 0.08 |
| PN406 | 2.3 ± 0.3* | 0.76 ± 0.03 |
| PN715 | 7.2 ± 3.9* | 0.84 ± 0.17 |

[a]The values are reported as mean ± SEM ($n$ = 3). Statistically significant differences are denoted with * (one-way ANOVA, $P$ < 0.05).

The one-way ANOVA analysis revealed a statistically significant difference for the $K_d$ values of all mutants compared to the wild-type peptide whereas the number of binding sites did not show a significant difference. In the presence of magnesium, which does not induce the $\beta$-roll secondary structure formation,[18,23,35] some reproducible temperature changes were observed upon lysozyme titration (independent of the mutations). However, the results were not comparable to what was observed with calcium and the data could not be fitted to yield binding parameters (Figure S3). Even though a buffer mis-match was not observed during the ITC experiments, it is possible that these heat changes were caused by a combination of heat of mixing and nonspecific binding by other residues of the peptides, which are not located on the $\beta$-roll faces. Of the 10 candidates investigated from the positive/negative selections, 7 were found to either behave similarly compared to the wild-type $\beta$-roll or to not demonstrate quantifiable affinity for the target, in the folded conformation (Figure S4).

**Characterization of Identified RTX Block V Mutants by Circular Dichroism (CD) Spectroscopy.** The responsiveness of the mutants to calcium was investigated by CD spectroscopy and it was observed that the responses to calcium were largely unaffected by the mutations. Figure 2A shows the CD spectra of the wild-type and the mutant peptides in the absence of calcium and the spectra in the presence of 10 mM $CaCl_2$ are shown in Figure 2B. In the absence of calcium, the CD spectra exhibited large negative peaks at 198 nm for all constructs, indicating a lack of secondary structure (Figure 2A). In the presence of calcium, the minima shifted to 218 nm, indicating the transition from unstructured peptide to $\beta$-sheet structure for every mutant (Figure 2B). For the wild-type and the PN406 mutant peptides, calcium titrations were performed up to 10 mM $CaCl_2$ (Figure 2C). The data were fit to the Hill equation to determine the calcium binding parameters (Figure 2D). PN406 bound calcium with a similar affinity compared to the wild-type and Hill coefficients greater than 1 indicated cooperative binding between the peptides and the calcium ions.

**Combined Binding Interfaces For Improved Apparent Affinity.** To improve target binding, combined $\beta$-roll interfaces



DOI: 10.1021/acssynbio.7b00089
ACS Synth. Biol. XXXX, XXX, XXX−XXX

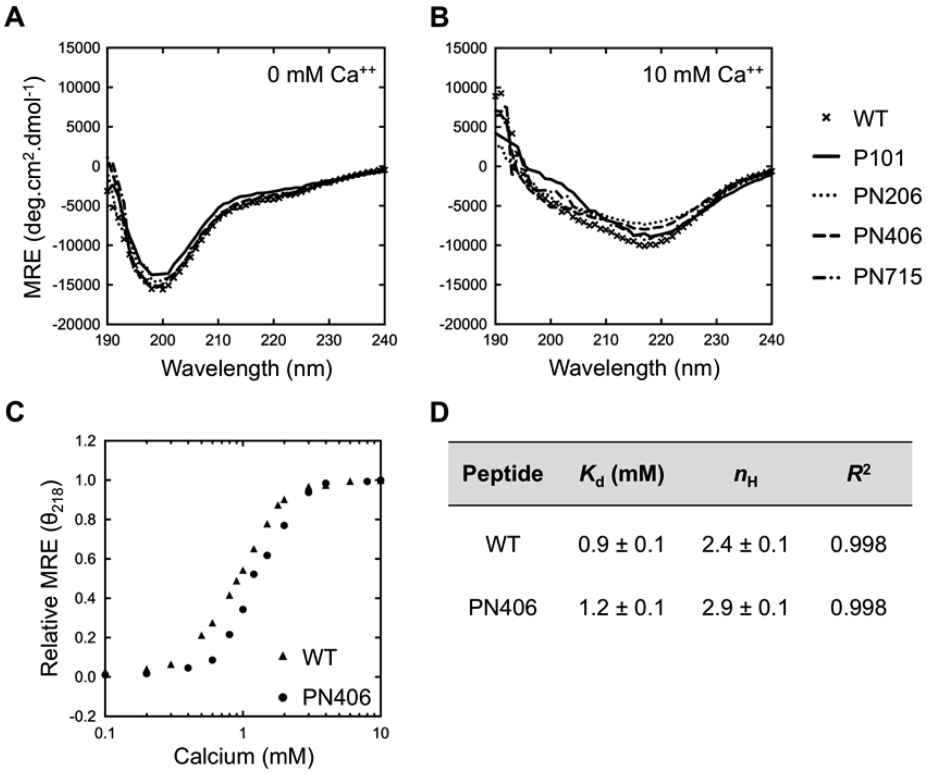


| Peptide | $K_d$ (mM) | $n_H$ | $R^2$ |
|---|---|---|---|
| WT | 0.9 ± 0.1 | 2.4 ± 0.1 | 0.998 |
| PN406 | 1.2 ± 0.1 | 2.9 ± 0.1 | 0.998 |

**Figure 2.** Characterization of $\beta$-rolls with Circular Dichroism Spectroscopy (CD). Mean residue ellipticity (MRE) was recorded over a range of wavelengths for wild-type as well as mutant RTX sequences (A) in the absence and (B) in the presence of 10 mM $CaCl_2$. (C) Recorded relative MRE (at 218 nm) at different calcium concentrations for wild-type RTX and PN406. (D) The data were fit to the Hill equation using nonlinear regression software and the obtained calcium binding parameters are reported (mean ± SEM, $n$ = 3).

were explored. A concatemer of PN406 was created by fusing the same genes in series: PN406-PN406. The binding surface area was further increased by inserting a third PN406 gene to this construct: PN406-PN406-PN406. Four additional concatemers were created by fusing the single mutants PN206 and PN715 to PN406. In addition, the opposite face of the folded $\beta$-roll was explored by mutating the eight residues on the back face to contain the amino acid residues of PN406: PN406/PN406. The resulting mutant had the same mutations on both faces. Lastly, the binding suitability of the back face of the $\beta$-roll was explored by itself. The eight residues on the front face of PN406/PN406 were reverted back to the wild-type residues: WT/PN406. Illustrations of the designed tertiary structures are shown in Figure 3A with their mutated residues presented in green.

The concatenated and double-face mutants were analyzed *via* ITC. Multiple copies of a binding interface can introduce an avidity effect leading to a higher apparent affinity and this was explored by concatenating different RTX mutants. Even though the single mutants had similar affinities, different combinations of them led to significant differences in overall binding parameters. The binding parameters of the combined $\beta$-roll mutants are reported in Table 2. The concatemer with highest affinity was found to be PN406-PN406, which bound lysozyme with an apparent dissociation constant of 65 nM and the insertion of another PN406 to this construct (PN406-PN406-PN406, $K_{d,apparent}$ = 155 nM) did not further improve the avidity. The number of binding sites was higher for some of the concatemers, indicating more of a 1:1 interaction between the mutants and lysozyme. Since lysozyme is able to form dimers,[36,37] it is not clear if the improvement in apparent affinity is due to avidity or due to binding of the dimeric form of the target enzyme. The latter case could explain why the monomeric mutants had binding site numbers closer to 0.5 (indicating 2 mutants binding per lysozyme) and the addition of a third PN406 to PN406-PN406 does not improve the apparent affinity any further.

The $\beta$-roll domains appear to be symmetrical by inspection of their primary sequences, such that amino acids project out radially from faces on both sides of the $\beta$-roll domain (Figure 1B). By placing the mutant amino acids on the backside of the domain, we explored if the binding face could be transplanted to the other side of the scaffold. Similar dissociation constants were observed for WT/PN406 and WT $\beta$-roll and for PN406/PN406 and PN406 (Table 2), suggesting that the residues on the other face of the peptide did not contribute to the overall interaction. This is likely due to the fact that the two faces of the RTX peptide used in this work are in fact not symmetrical and that the second face of the $\beta$-roll has a more concave structure compared to the other face (Figure 1B). The capping group is also not symmetrical and could add steric hindrance on the backside of the $\beta$-roll that prevents lysozyme binding by the selected amino acids.

For all $\beta$-roll mutants, the change in the Gibbs free energy of binding upon interaction with lysozyme was calculated (Figure 3B, Table S4). The largest difference was observed in PN406-PN406 (−10.1 kcal/mol), followed by triple-PN406 (−9.4 kcal/mol). Among the 8 mutations, positions 1, 3, 4, and 5 were dominated by the hydrophobic residues (Figure S5). The raw and fitted ITC data for wild-type, PN406 and PN406-PN406 are presented in Figure 4A, B and C, respectively. Control experiments were performed in the presence of


DOI: 10.1021/acssynbio.7b00089
ACS Synth. Biol. XXXX, XXX, XXX−XXX

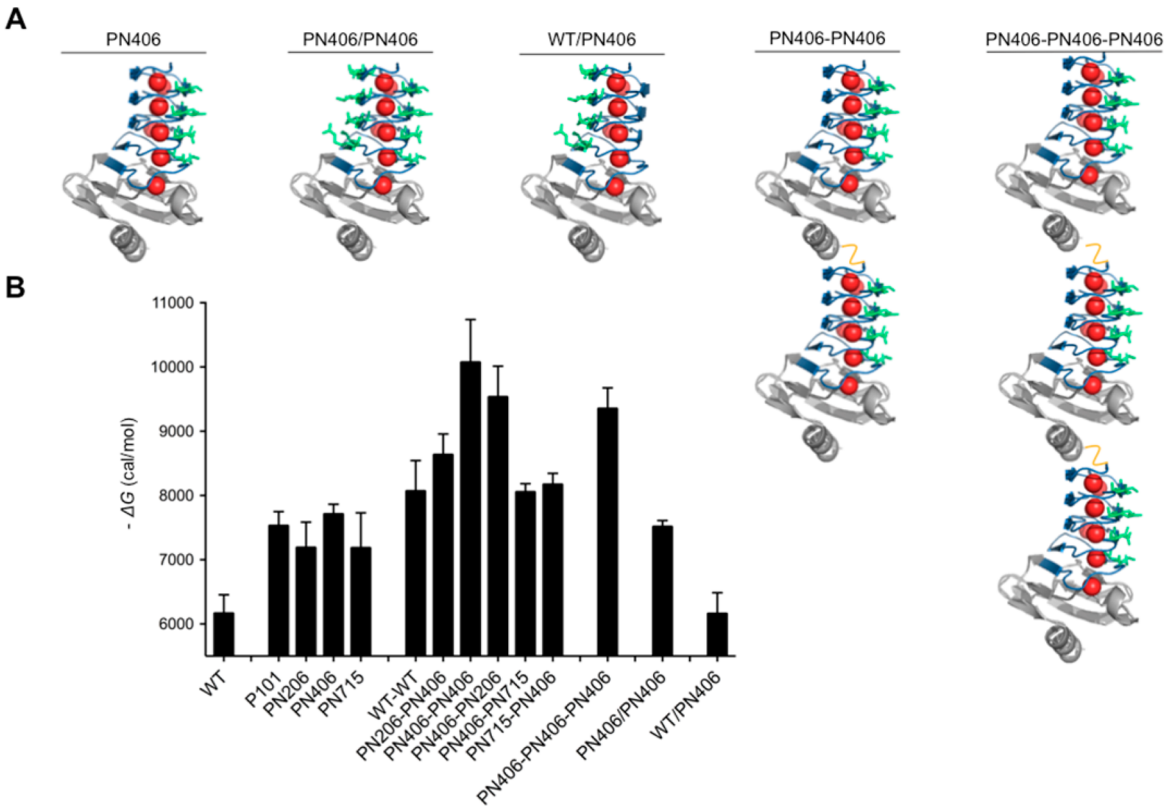


**Figure 3.** Designed RTX mutants and changes in the Gibbs free energy upon lysozyme binding. (A) Illustrations of the designed tertiary structures of mutants genetically constructed based on PN406. The mutated residues are shown in green. Calcium ions and the linker between concatamers are shown in red and yellow, respectively. PN406/PN406 has the mutated residues on both faces and WT/PN406 has mutated residues only on the opposite face. PN406-PN406 and PN406-PN406-PN406 are the concatenated mutants. (B) Changes in the Gibbs free energy upon interacting with lysozyme. The error bars denote the SD ($n$ = 3).

**Table 2. Binding Parameters of Concatenated and Double-Face Peptides**[a]

| peptide | apparent dissociation constants ($K_{d,apparent}$) | number of binding sites ($N$) |
|---|---|---|
| WT-WT | 1.4 ± 0.5 $\mu$M | 0.80 ± 0.04 |
| PN206-PN406 | 514 ± 155 nM* | 0.57 ± 0.13 |
| PN406-PN206 | 122 ± 42 nM* | 0.58 ± 0.03 |
| PN406-PN406 | 65 ± 28 nM* | 0.79 ± 0.04 |
| PN406-PN715 | 1.3 ± 0.2 $\mu$M | 1.07 ± 0.03 |
| PN715-PN406 | 1.0 ± 0.2 $\mu$M | 1.12 ± 0.11* |
| PN406-PN406-PN406 | 155 ± 54 nM* | 1.05 ± 0.08 |
| PN406/PN406 | 3.1 ± 0.3 $\mu$M* | 1.17 ± 0.06* |
| WT/PN406 | 34 ± 10 $\mu$M | 0.82 ± 0.01 |

[a]The values are reported as mean ± SEM ($n$ = 3). Statistically significant differences are denoted with * (one-way ANOVA, $P$ < 0.05).

magnesium and no binding signal was observed. The raw ITC data of PN406-PN406 in the presence of magnesium did not demonstrate any binding signal (Figure S3C).

***In Vitro* Demonstration of Molecular Recognition Regulation *via* Affinity Chromatography.** Allosterically controlled biomolecular recognition scaffolds should benefit many biotechnology applications. To demonstrate the control over the binding behavior, the $\beta$-roll mutant with the highest affinity was utilized in the "catch and release" affinity chromatography purification of lysozyme. The concatemer of PN406 was fused to maltose binding protein (MBP), was immobilized on columns and the capture of the target molecule, lysozyme, was assessed in the presence of either calcium or magnesium. A schematic of the chromatography experiments is shown in Figure 5. Following target loading, columns were washed for 10 column volumes (CVs, 1 CV = 5 mL) with buffer modified with calcium or magnesium. Subsequently, the columns were washed for 20 CVs (100 mL) with regular column buffer, which did not contain calcium or magnesium. The same experiments were repeated with the WT-WT fused to MBP, as a negative control.

Figure 6A shows affinity chromatography data for PN406-PN406 and WT-WT. Only the mutant peptide was capable of forming sufficient interactions with lysozyme to capture it in the presence of calcium. Area under the curve analysis showed that, in the case of PN406-PN406/$Ca^{2+}$, 66% of the loaded lysozyme was recovered within the first 50 mL of the elution step. At the peak fractions during column wash, the recovered lysozyme amount was 75% for WT-WT/$Mg^{2+}$, 78% for WT-WT/$Ca^{2+}$ and 74% for PN406-PN406/$Mg^{2+}$, all of which could not capture the target molecule. Chromatography peak fractions were analyzed *via* sodium dodecyl sulfate polyacrylamide gel electrophoresis (SDS-PAGE) and the resulting bands corresponded to lysozyme, which has a molecular weight of 14.3 kDa. Identical experiments were performed with fluorescein isothiocyanate (FITC)-labeled lysozyme (Figure 6B). After washing the columns for 10 CVs (50 mL), the columns were visualized under UV light to detect the FITC label. As shown in Figure 6B, only PN406-PN406 was capable of retaining the target, in the presence of calcium. To test the


DOI: 10.1021/acssynbio.7b00089
ACS Synth. Biol. XXXX, XXX, XXX−XXX

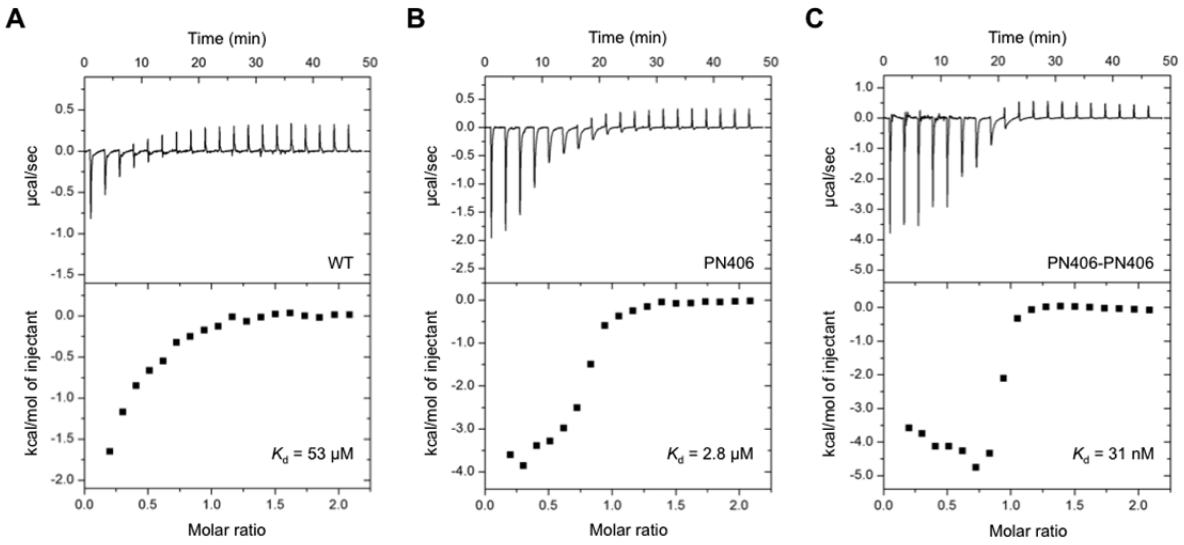


**Figure 4.** Lysozyme binding characteristics in the presence of calcium. (A–C) ITC data for titration of lysozyme into wild-type RTX, PN406 and PN406-PN406. The raw data is presented in the upper panels and bottom panels show the integrated data fitted *via* one-site binding model.

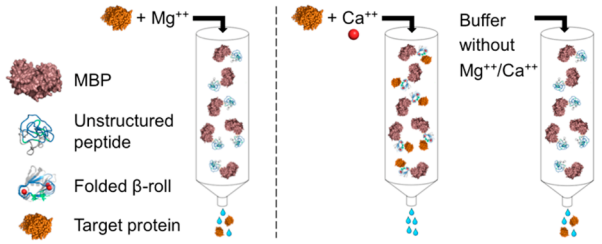


**Figure 5.** Cartoon representation of the affinity chromatography experiments. PN406-PN406 mutant was genetically fused to maltose binding protein (MBP) and immobilized on resin. In the presence of magnesium, the mutant peptides remain unstructured. In the presence of calcium (middle panel) the $\beta$-rolls fold and retain the target molecule on the column. The last panel shows the elution step where the calcium ions are washed away. The $\beta$-rolls transition to their unfolded state, losing interaction with the target.

recyclability of the capture and release, the same column was used for three rounds of target loading and elution.

Lastly, the selectivity of the interactions between PN406-PN406 and lysozyme was investigated. Similar affinity chromatography experiments were performed where lysozyme was mixed with *E. coli* crude cell lysate (200 and 1000 $\mu$L) prior to sample loading (Figure 7). The lysozyme sample mixed with the 1000 $\mu$L of lysate was chosen to mimic a realistic high-level recombinant protein expression system were the lysozyme product would constitute 40 wt % of the total cellular protein loaded on the column. The *E. coli* proteins were found to elute during the column wash whereas the lysozyme was eluted after the calcium ions were eliminated (following the switch in the column buffer). 65% and 60% of the loaded lysozyme were recovered within the first 50 mL of the elution step, for the samples with 200 and 1000 $\mu$L of cell lysate, respectively. Lane 6 in the SDS-PAGE gel picture shows the purified, active lysozyme (Figure S6) whereas the peak fraction of the column wash containing the nonspecific *E. coli* proteins is shown in lane 5.

Nanomolar affinities appear to be sufficient for the RTX peptide to be used in affinity chromatography applications. In most of the affinity-based approaches, target elution can be challenging. For example, in immunochromatography methods, large pH swings or high concentrations of chemical denaturants are required to disrupt the interactions between the target and the antibody.[38,39] The use of the engineered RTX peptide provides an easy elution step by taking advantage of environmental control over the structure of the scaffold. The $K_d$ of the $\beta$-roll for calcium (~1 mM) allows the elution of the target without the need for a chelator. In addition, the results shown in Figure 6B demonstrate the reusability of this catch and release platform as the binding interface can be regenerated and reused. In addition to bioseparations, this switchable binding platform can be suitable for other biotechnology applications including biosensors, protein scaffolding, and protein immobilization. Another interesting potential feature to be investigated could involve separate evolution of the two $\beta$-roll faces in the same peptide. If each face demonstrates an affinity for different targets, the capacity of this platform could be exploited for a variety of studies involving protein assembly.

In conclusion, we explored whether the RTX sequence, which exhibits disordered-to-ordered transition but it is not known to participate in biomolecular recognition, could be engineered to create a novel binding interface specifically controlled by the presence of calcium. By selecting RTX mutants that conditionally bind the lysozyme target, which has been a model target in directed evolution research, we have begun to explore the idea of controllable supramolecular assembly and conformationally dependent ligand capture. The disordered-to-ordered transition of the RTX domain serves as a switch for turning the binding on and off. The reversibility of calcium binding allows the engineered molecular recognition to be controllable and thus, calcium-triggered target "catch and release" can be achieved. While the applicability of the approach demonstrated here to targets other than lysozyme remains to be investigated, our studies demonstrate the feasibility of using conformationally dynamic or instrinsically disordered motifs in biomolecular recognition, which has been largely unexplored, and may assist the rational design of future stimulus-responsive scaffolds to carry out controllable molecular recognition playing an important role in many biological processes.


DOI: 10.1021/acssynbio.7b00089
*ACS Synth. Biol.* XXXX, XXX, XXX–XXX

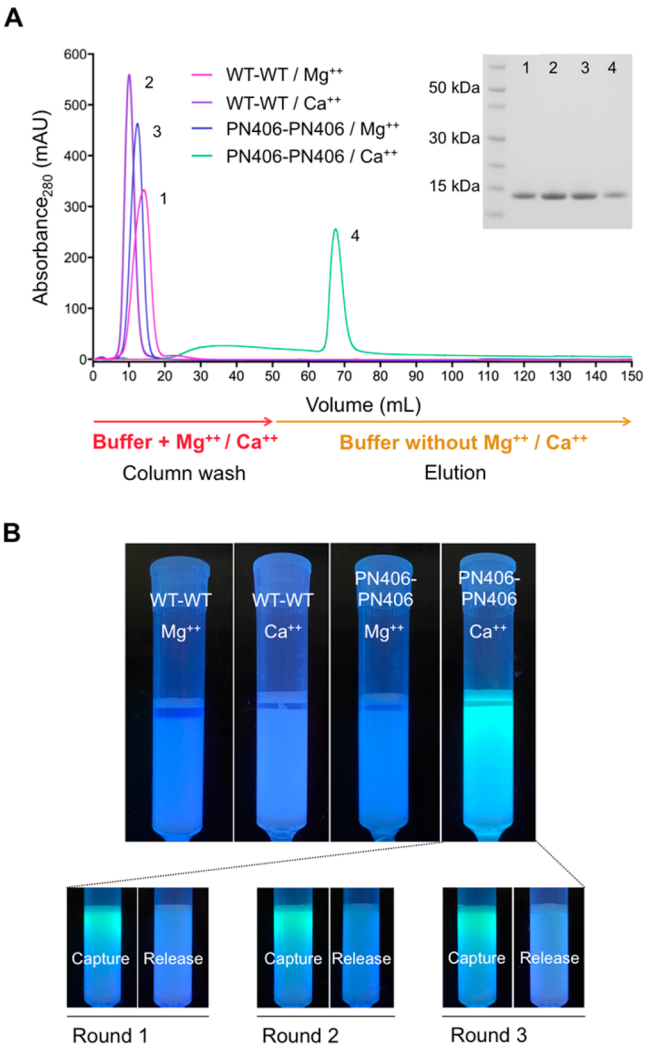


**Figure 6.** Demonstration of control over biomolecular recognition *via* allosteric regulation. (A) Affinity chromatography experiments performed with immobilized MBP-WT-WT and MBP-PN406-PN406. The absorbance at 280 nm was recorded for four different runs: each protein was tested in the presence of calcium or magnesium. After lysozyme loading, the columns were washed with buffer containing $Ca^{2+}$ or $Mg^{2+}$. Elution was performed using buffer without $Ca^{2+}$ or $Mg^{2+}$. The lysozyme was eluted during the column wash for WT-WT/$Mg^{2+}$, WT-WT/$Ca^{2+}$ and PN406-PN406/$Mg^{2+}$. It was eluted from PN406-PN406/$Ca^{2+}$ only after calcium was removed. The SDS-PAGE gel picture shows the samples taken from the peak fractions of each curve; the molecular weight of lysozyme is 14.3 kDa. (B) Identical experiments were performed with FITC-labeled lysozyme. Column pictures were taken under UV-light to detect any FITC presence. Green color indicates the lysozyme captured by PN406-PN406 in the presence of $Ca^{2+}$. The bottom panel presents the capture and release cycles conducted with the same column.

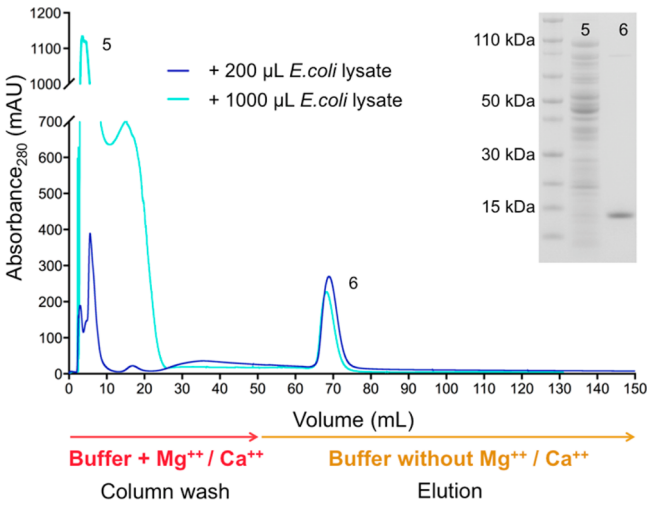


**Figure 7.** Selectivity of the target capture. Affinity chromatography experiments performed with immobilized MBP-PN406-PN406 where lysozyme was mixed with *E. coli* crude cell lysate. PN406-PN406 captured the lysozyme from the *E. coli* crude cell lysate matrix. Lane 5 in the gel picture shows the *E. coli* lysate proteins which did not bind to the column. Lane 6 shows the purified lysozyme, which was released upon the switch to the $Ca^{2+}$-free buffer.

## MATERIALS AND METHODS

**Plasmids and Chemicals.** Block V RTX domain and the capping group were amplified from the pDLE9-CyaA plasmid, a gift from Dr. Daniel Ladant (Institute Pasteur, Paris), as described before.[35,40] The intein domain from pET-EI/OPH[41] was a gift from Dr. David Wood (Ohio State University, Columbus, OH). The ribosome display vector (pRDV, GenBank AY327136.1) was a gift from Dr. Andreas Plückthun (University of Zurich, Zurich).[42,43] Restriction enzymes for cloning experiments, amylose resin and the PURExpress protein synthesis kit were purchased from New England Biolabs. Preblocked streptavidin coated plates and the RETROscript reverse transcription kit were purchased from Thermo Fisher Scientific. The RNeasy mini kit was purchased from QIAGEN. Isopropyl $\beta$-D-1-thiogalactopyranoside (IPTG) and ampicillin sodium salt, were purchased from Gold Biotechnology. Amicon centrifugal filters were purchased from Millipore. Sodium dodecyl sulfate polyacrylamide electrophoresis gels (SDS-PAGE) and running buffers were purchased from Invitrogen-Life Technologies. All oligonucleotides were purchased from Integrated DNA Technologies. *E. coli* 5-alpha cell line was purchased from Bioline. Terrific broth media for protein expression and FITC-labeled lysozyme were purchased from Thermo Fisher Scientific. All other reagents and materials were purchased from Sigma-Aldrich unless otherwise stated.

**Library Construction.** The randomized RTX peptide library was constructed using two, overlapping oligonucleotides encoding for the entire gene. Randomized positions were created at the DNA level using degenerate codons. NNK bases were inserted at eight selected positions, forming a randomized face in the folded conformation. N represents any base, A, T, C or G. K represents the keto-containing bases, G or T. This codon stretch can code for all 20 common amino acids while simultaneously knocking out two *E. coli* RNA stop codons, ochre (UAA) and umber (UGA). The library oligonucleotides were annealed and extended creating full-length, hybridized library. The C-terminal capping region was then added to the library by overlap extension PCR. All oligonucleotide sequences for the library construction and capping can be found in the Table S5.

**Selection of Mutants *via* Ribosome Display.** The capped RTX peptide library was subcloned into pRDV using *Kpn*I and *Hin*dIII endonuclease restriction sites. The pRDV construct contains all of the genetic components required for cell-free transcription and translation including a T7 promoter and a ribosome binding site. The gene for an unstructured portion of the endogenous *E. coli* tolA protein lies directly downstream of the RTX library in pRDV (Figure S1). The sole


DOI: 10.1021/acssynbio.7b00089
ACS Synth. Biol. XXXX, XXX, XXX−XXX

function of this protein is to act as a spacer and allow the translated RTX variant to exit the ribosomal tunnel and fold in solution. Primers were designed to amplify the capped RTX library along with a portion of the tolA spacer (T7B and tolAK). A stop codon was excluded from this amplification to anchor the nascent protein and cognate mRNA strand to the ribosome, thereby maintaining a genotype-phenotype linkage.

250 ng of this PCR product was used as template for *in vitro* transcription and translation using the PURExpress system, according to the manufacturer's protocol. A 25 $\mu$L reaction was incubated for 1 h at 37 °C and terminated by adding 475 $\mu$L of ice-cold stop buffer (50 mM Tris−HCl, 150 mM NaCl, 0.1% (v/v) Tween 20, 2.5 mg mL$^{-1}$ heparin, pH 7.5). The mixture was centrifuged at 14 000*g* for 10 min to pellet insoluble reaction components. The soluble fractions from two reactions were isolated, combined and used immediately for selection ($10^{12}$ possible DNA transcripts, ignoring any amplification bias in the PCR step). Simultaneously, 100 $\mu$L of biotinylated lysozyme (∼350 $\mu$M) was immobilized on preblocked streptavidin coated microtiter plates for 1 h on an orbital shaker at 4 °C. The wells were washed three times with ice-cold wash buffer (50 mM Tris−HCl, 150 mM NaCl, 0.1% (v/v) Tween 20, pH 7.5), and used immediately for selection experiments. 150 $\mu$L of the clarified translation mix was added to each well containing immobilized lysozyme. The calcium or magnesium concentration was adjusted to 25 mM to ensure the RTX peptide remained folded or unstructured, respectively, during the biopanning process. Selections were carried out for 1 h at 4 °C on an orbital shaker. Unbound and weakly associated clones were removed from the well by washing with 300 $\mu$L of ice-cold wash buffer supplemented with either 25 mM $CaCl_2$ or $MgCl_2$. For initial rounds of selection, fewer washes were used (∼1−3). The stringency was increased for later rounds of selection in order to intensify the selective pressure on the RTX library (∼5−10). After the final wash, bound complexes were dissociated in 100 $\mu$L of elution buffer (50 mM Tris acetate, 150 mM NaCl, 25 mM EDTA, pH 7.5) for 5 min at 4 °C. The wells were washed with an additional 100 $\mu$L of elution buffer for 5 min at 4 °C to ensure high recovery. Recovered mRNA was purified on the QIAGEN RNeasy purification mini kit, according to the manufacturer's protocol, and used as template for reverse transcription using the RETROscript reverse transcription kit. The resultant cDNA was used as template to amplify the selected library for cloning back into pRDV for a subsequent round of selection. Individual library variants were screened by transforming pRDV into 5-alpha *E. coli*, isolating single colonies on selective agar plates, and sequencing the extracted plasmid DNA.

**Cloning of Mutants into Expression Plasmids and Construction of Concatemers.** The genes coding for mutant peptides were cloned into pMAL-intein backbone using the *Kpn*I and *Hin*dIII restriction sites. For the concatemer construction, first mutant was cloned into the same vector *via* *Kpn*I and *Hin*dIII sites, which did not have a stop codon at the C-terminus. The second mutant, with a stop codon at the end of the gene, was inserted *via* the *Hin*dIII site. For the triple mutant PN406-PN406-PN406, the third PN406 was inserted *via* *Kpn*I site into the pMAL-intein-PN406-PN406 backbone. Ten amino acid linker GGGGSGGGGS was included in between the mutants. For affinity chromatography experiments, concatemers of WT $\beta$-roll and PN406 were genetically fused to N terminus of maltose binding protein (MBP). For the construction of MBP-WT-WT, the first WT $\beta$-roll was inserted *via* *Ava*I and *Eco*RI sites and the second one was inserted *via* *Eco*RI and *Bam*HI sites, into the pMAL-c4e backbone. For MBP-PN406-PN406, the concatemer was amplified out of the pMAL-intein-PN406-PN406 plasmid and inserted into pMAL-c4e *via* *Ava*I and *Eco*RI sites. Resulting plasmids were transformed into 5-alpha cells. Corresponding primer sequences used during the PCR reactions are given in Table S5.

**Construction of Double Face Mutants.** For the construction of PN406/PN406, pMAL-intein-PN406 plasmid was used as the template. Eight residues on the other face of the mutant were mutated to the residues of PN406 by performing site-directed mutagenesis *via* QuikChange II Site-Directed Mutagenesis Kit (Agilent), so that both faces of the $\beta$-roll contained the residues of PN406. For the construction of WT/PN406, pMAL-intein-WT$\beta$-roll plasmid was used as the template and eight residues on the opposite face were mutated to contain the PN406 residues *via* site-directed mutagenesis. Corresponding primer sequences used during the PCR reactions are given in Table S6.

**Expression and Purification of WT and Mutant RTX Peptides.** The protein primary sequences of all peptides are given in Table S7. All constructs were expressed in 1 L of sterilized Terrific Broth supplemented with 100 $\mu$g mL$^{-1}$ ampicillin, 2 g L$^{-1}$ D-glucose and inoculated with 10 mL overnight culture. The cells were grown to an OD600 of 0.6 while shaking at 37 °C and protein expression was induced with 0.3 mM IPTG. Expression was carried out for 4−5 h at 37 °C. Cells were harvested by centrifugation at 5000 *g* for 10 min and resuspended in 50 mL MBP column buffer (20 mM Tris-HCl, 200 mM NaCl, 1 mM EDTA, pH 7.4) per L of culture. For affinity chromatography experiments, modified MBP column buffer was used, which did not contain EDTA. Cells were lysed *via* sonication with an ultrasonication probe in ice bath for 6 min (5 s on pulse and 2 s off pulse). The lysed cell suspension was centrifuged at 15 000*g* for 30 min and the soluble fraction was collected. For the purification of all proteins in fusion with MBP-intein, columns packed with amylose resin were used. The cell lysate was diluted to a volume of 200 mL, loaded onto equilibrated amylose columns and the columns were washed with the MBP column buffer. Then, the columns were saturated with intein cleaving buffer (137 mM NaCl, 2.7 mM KCl, 8.1 mM $Na_2HPO_4$, 1.76 mM $KH_2PO_4$, 40 mM bis-Tris, 2 mM EDTA, pH 6.2), capped and incubated at 37 °C for 16−20 h. Cleaved proteins were eluted with 50 mL of MBP column buffer. Amicon filters with 10 or 30 kDa molecular weight cutoff were used in order to concentrate the protein solutions as well as to buffer exchange into Q column low salt buffer (20 mM bis-Tris, 25 mM NaCl, pH 6.0). The concentrated and buffer exchanged protein samples were loaded onto 16/10 QFF ion exchange column (GE Healthcare). Target proteins were eluted using a linear NaCl gradient from 25 mM to 500 mM NaCl. Chromatography fractions were run on SDS-PAGE and pure fractions were combined and concentrated. For the affinity chromatography experiments, MBPTrap (GE Healthcare) columns were used. Cell lysates containing MBP fusion proteins were loaded onto the columns and the columns were washed with the modified MBP column buffer to remove any other nonspecifically bound proteins.

**Circular Dichroism (CD) Spectroscopy.** Protein samples were buffer exchanged into 50 mM Tris, pH 7.4. 0.1 mm path length quartz cuvette was used in order to analyze the peptides. 100 $\mu$M protein samples were incubated with 10 mM $CaCl_2$ and were analyzed on a J-815 CD spectrometer (Jasco).


DOI: 10.1021/acssynbio.7b00089
ACS Synth. Biol. XXXX, XXX, XXX−XXX

Calcium titration ($CaCl_2$ concentration varying between 0−10 mM) was performed with WT $\beta$-roll and PN406. The data was fit to the Hill equation using SigmaPlot software.

**Isothermal Titration Calorimetry (ITC).** All constructs were analyzed *via* MicroCal Auto-iTC200 in order to assess their binding parameters. In each experiment, 350 $\mu$M RTX peptide and 3.5 mM hen egg white lysozyme were used. The lysozyme was dissolved in 50 mM Tris, pH 7.4, modified with 10 mM $CaCl_2$ or $MgCl_2$ and dialyzed against the same buffer, overnight prior to ITC experiments. All experiments were carried out at 25 °C. Titrations were conducted by 19 identical injections of 2 $\mu$L with duration of 4 s per injection and a spacing of 150 s between injections. The collected data were analyzed with the MicroCal Origin software supplied with the instrument to determine the binding constants *via* one-site model. At least three ITC runs were performed for each construct. The resulting binding parameters were statistically analyzed *via* one-way ANOVA, where mutants were compared to either WT $\beta$-roll or concatenated WT-WT.

**Affinity Chromatography Experiments.** The chromatography data presented in Figures 6 and 7 involved two different constructs, MBP-WT-WT and MBP-PN406-PN406. Four MBP-Trap columns were used in total (two for each fusion protein for two different salt conditions). For all chromatography experiments, the assay buffer (MBP column buffer) did not contain any EDTA. Diluted cell lysates (5 mL) were loaded onto the columns after the columns were equilibrated with MBP column buffer. The columns were washed with 100 mL of MBP column buffer and equilibrated with 50 mL of MBP column buffer modified with either 10 mM $CaCl_2$ or $MgCl_2$. After the equilibration, 1 mL of concentrated lysozyme solution (in the same modified MBP column buffer) was loaded onto the columns (accurate amounts: 4.37 and 4.60 mg for $CaCl_2$ and $MgCl_2$ runs, respectively). The columns were washed with 50 mL of modified MBP column buffer. Then, 100 mL of regular MBP column buffer (no calcium or magnesium) was run through the columns in order to wash away the ions and to elute the bound lysozyme. For FITC-labeled lysozyme experiments (Figure 6B), the experimental setup was the same as described above except columns prepacked with amylose resin were used instead of the MBP-Trap columns. Columns were visualized under the UV light box to detect the FITC presence. For the specificity experiments, same amount of lysozyme (4.37 mg) was coloaded with 200 or 1000 $\mu$L *E. coli* cell lysate, in the presence of calcium. For these experiments, BL21(DE3) cell lines were grown and cell lysate containing *E. coli* proteins were obtained after sonication of the resuspended cell pellets (1 L cell culture in 40 mL buffer) followed by centrifugation of lysed cells. Area under the curve calculations were done *via* Matlab software where trapz(x,y) function was used to calculate the protein amounts.

**Activity Assay of Lysozyme.** Enzymatic activity of the eluted lysozyme fractions was assayed *via* Enzymatic Assay of Lysozyme kit (Sigma-Aldrich). Briefly, a cell suspension (0.01% (w/v)) was prepared by dissolving lyophilized *Micrococcus lysodeikticus* in the assay buffer (66 mM potassium phosphate buffer, pH 6.24). In a UV cuvette, 2.5 mL of the cell suspension was mixed with 0.1 mL of the lysozyme fraction to be tested and the decrease in absorbance at 450 nm was recorded for a time interval of 5 min.

**Statistical Analysis.** All experiments were performed in triplicates. One-way ANOVA analysis was applied to the ITC results to compare the number of binding sites and dissociation constant values of single mutants (P101, PN206, PN406 and PN715) and double face mutants (WT/PN406 and PN406/PN406) to wild-type $\beta$-roll and to compare the number of binding sites and dissociation constant values of concatenated mutants (PN206-PN406, PN406-PN206, PN406-PN406, PN406-PN715, PN715-PN406 and PN406-PN406-PN406) to the concatemer of wild-type $\beta$-roll.

## ■ ASSOCIATED CONTENT

### Supporting Information

The Supporting Information is available free of charge on the ACS Publications website at DOI: 10.1021/acssynbio.7b00089.

Supplementary Figures: Schematic of the ribosome display selection method, SDS-PAGE analysis of WT and mutant peptides, Exemplary ITC analysis of WT, PN406 and PN406-PN406-PN406 in the presence of magnesium, Exemplary ITC analysis of PN316 and PN708 in the presence of calcium, Activity assay of the eluted lysozyme; Supplementary Tables: Sequencing results of the positive selections, Sequencing results of the positive/negative selections, Selected mutants from the positive/negative selections, The changes in the Gibbs free energy upon interaction with lysozyme, PCR primers for cloning experiments, PCR primers for site-directed mutagenesis experiments, Protein primary sequences (PDF)

## ■ AUTHOR INFORMATION


### Corresponding Author

*E-mail: sbanta@columbia.edu. Tel: +1 212-854-7531.

### ORCID

Scott Banta: 0000-0001-7885-0150

### Present Addresses

[†]Codiak BioSciences, Cambridge, Massachusetts 01801, United States.

[‡]VTT Technical Research Centre of Finland Ltd., Espoo 02044, Finland.

[§]Department of Chemical and Biomolecular Engineering, Clemson University, Clemson, South Carolina 29634, United States.


### Author Contributions

B.B., K.D., G.S., M.B. and S.B. conceived the concept. B.B. and K.D. designed and performed the experiments. S.B. directed the research. B.B. and K.D. wrote the manuscript, and all authors provided feedback on the manuscript.

### Notes

The authors declare no competing financial interest.

## ■ ACKNOWLEDGMENTS

The authors gratefully acknowledge financial support from the US National Science Foundation (1161160 and 1402656), the Defense Threat Reduction Agency (CB2819 BRCALL07-E-2-0035), the U.S. Army 6.1 Basic Research Program (W9132T-08-2-0002) and the Academy of Finland.

## ■ REFERENCES

(1) Hoogenboom, H. R. (2005) Selecting and screening recombinant antibody libraries. *Nat. Biotechnol. 23*, 1105−1116.

(2) Alt, F. W., Blackwell, T. K., and Yancopoulos, G. D. (1987) Development of the primary antibody repertoire. *Science 238*, 1079−1087.



DOI: 10.1021/acssynbio.7b00089
*ACS Synth. Biol.* XXXX, XXX, XXX−XXX

(3) Boder, E. T., Midelfort, K. S., and Wittrup, K. D. (2000) Directed evolution of antibody fragments with monovalent femtomolar antigen-binding affinity. *Proc. Natl. Acad. Sci. U. S. A. 97*, 10701−10705.
(4) Hey, T., Fiedler, E., Rudolph, R., and Fiedler, M. (2005) Artificial, non-antibody binding proteins for pharmaceutical and industrial applications. *Trends Biotechnol. 23*, 514−522.
(5) Binz, H. K., Amstutz, P., and Plückthun, A. (2005) Engineering novel binding proteins from nonimmunoglobulin domains. *Nat. Biotechnol. 23*, 1257−1268.
(6) Skerra, A. (2007) Alternative non-antibody scaffolds for molecular recognition. *Curr. Opin. Biotechnol. 18*, 295−304.
(7) Banta, S., Dooley, K., and Shur, O. (2013) Replacing antibodies: Engineering new binding proteins. *Annu. Rev. Biomed. Eng. 15*, 93−113.
(8) Löfblom, J., Feldwisch, J., Tolmachev, V., Carlsson, J., Ståhl, S., and Frejd, F. Y. (2010) Affibody molecules: Engineered proteins for therapeutic, diagnostic and biotechnological applications. *FEBS Lett. 584*, 2670−2680.
(9) Binz, H. K., Stumpp, M. T., Forrer, P., Amstutz, P., and Plückthun, A. (2003) Designing repeat proteins: Well-expressed, soluble and stable proteins from combinatorial libraries of consensus ankyrin repeat proteins. *J. Mol. Biol. 332*, 489−503.
(10) Kobe, B., and Kajava, A. V. (2001) The leucine-rich repeat as a protein recognition motif. *Curr. Opin. Struct. Biol. 11*, 725−732.
(11) Goh, C. S., Milburn, D., and Gerstein, M. (2004) Conformational changes associated with protein-protein interactions. *Curr. Opin. Struct. Biol. 14*, 104−109.
(12) Ostermeier, M. (2005) Engineering allosteric protein switches by domain insertion. *Protein Eng., Des. Sel. 18*, 359−364.
(13) Ambroggio, X. I., and Kuhlman, B. (2006) Design of protein conformational switches. *Curr. Opin. Struct. Biol. 16*, 525−530.
(14) cChockalingam, K., Blenner, M., and Banta, S. (2007) Design and application of stimulus-responsive peptide systems. *Protein Eng., Des. Sel. 20*, 155−161.
(15) Uversky, V. N., Oldfield, C. J., and Dunker, A. K. (2008) Intrinsically disordered proteins in human diseases: Introducing the D2 concept. *Annu. Rev. Biophys. 37*, 215−246.
(16) Dyson, H. J., and Wright, P. E. (2005) Intrinsically unstructured proteins and their functions. *Nat. Rev. Mol. Cell Biol. 6*, 197−208.
(17) Oldfield, C. J., Meng, J., Yang, J. Y., Yang, M. Q., Uversky, V. N., and Dunker, A. K. (2008) Flexible nets: Disorder and induced fit in the associations of p53 and 14−3-3 with their partners. *BMC Genomics 9*, S1.
(18) Bauche, C., Chenal, A., Knapp, O., Bodenreider, C., Benz, R., Chafotte, A., and Ladant, D. (2006) Structural and functional characterization of an essential RTX subdomain of *Bordetella pertussis* adenylate cyclase toxin. *J. Biol. Chem. 281*, 16914−16926.
(19) Lilie, H., Haehnel, W., Rudolph, R., and Baumann, U. (2000) Folding of a synthetic parallel $\beta$-roll protein. *FEBS Lett. 470*, 173−177.
(20) Rose, T., Sebo, P., Bellalou, J., and Ladant, D. (1995) Interaction of calcium with *Bordetella pertussis* adenylate cyclase toxin. *J. Biol. Chem. 270*, 26370−26376.
(21) Sotomayor-Pérez, A. C., Ladant, D., and Chenal, A. (2015) Disorder-to-order transition in the CyaA toxin RTX domain: Implications for toxin secretion. *Toxins 7*, 1−20.
(22) Bumba, L., Masin, J., Macek, P., Wald, T., Motlova, L., Bibova, I., Klimova, N., Bednarova, L., Veverka, V., Kachala, M., Svergun, D. I., Barinka, C., and Sebo, P. (2016) Calcium-driven folding of RTX domain $\beta$-rolls ratchets translocation of RTX proteins through type I secretion ducts. *Mol. Cell 62*, 47−62.
(23) Szilvay, G. R., Blenner, M. A., Shur, O., Cropek, D. M., and Banta, S. (2009) A FRET-based method for probing the conformational behavior of an intrinsically disordered repeat domain from *Bordetella pertussis* adenylate cyclase. *Biochemistry 48*, 11273−11282.
(24) Chenal, A., Karst, J. C., Sotomayor-Pérez, A. C., Wozniak, A. K., Baron, B., England, P., and Ladant, D. (2010) Calcium-induced folding and stabilization of the intrinsically disordered RTX domain of the CyaA toxin. *Biophys. J. 99*, 3744−3753.
(25) Chenal, A., Guijarro, J. I., Raynal, B., Delepierre, M., and Ladant, D. (2009) RTX calcium binding motifs are intrinsically disordered in the absence of calcium. *J. Biol. Chem. 284*, 1781−1789.
(26) Sotomayor-Pérez, A. C., Ladant, D., and Chenal, A. (2011) Calcium-induced folding of intrinsically disordered repeat-in-toxin (RTX) motifs *via* changes of protein charges and oligomerization states. *J. Biol. Chem. 286*, 16997−17004.
(27) Sotomayor-Pérez, A. C., Karst, J. C., Davi, M., Guijarro, J. I., Ladant, D., and Chenal, A. (2010) Characterization of the regions involved in the calcium-induced folding of the intrinsically disordered RTX motifs from the *Bordetella pertussis* adenylate cyclase toxin. *J. Mol. Biol. 397*, 534−549.
(28) De Genst, E., Silence, K., Decanniere, K., Conrath, K., Loris, R., Kinne, J., Muyldermans, S., and Wyns, L. (2006) Molecular basis for the preferential cleft recognition by dromedary heavy-chain antibodies. *Proc. Natl. Acad. Sci. U. S. A. 103*, 4586−4591.
(29) Hackel, B. J., Kapila, A., and Wittrup, K. D. (2008) Picomolar affinity fibronectin domains engineered utilizing loop length diversity, recursive mutagenesis, and loop shuffling. *J. Mol. Biol. 381*, 1238−1252.
(30) Odegrip, R., Coomber, D., Eldridge, B., Hederer, R., Kuhlman, P. A., Ullman, C., FitzGerald, K., and McGregor, D. (2004) CIS display: *In vitro* selection of peptides from libraries of protein-DNA complexes. *Proc. Natl. Acad. Sci. U. S. A. 101*, 2806−2810.
(31) Mariuzza, R. A., Velikovsky, C. A., Deng, L., Xu, G., and Pancer, Z. (2010) Structural insights into the evolution of the adaptive immune system: The variable lymphocyte receptors of jawless vertebrates. *Biol. Chem. 391*, 753−760.
(32) Blenner, M. A., Shur, O., Szilvay, G. R., Cropek, D. M., and Banta, S. (2010) Calcium-induced folding of a beta roll motif requires C-terminal entropic stabilization. *J. Mol. Biol. 400*, 244−256.
(33) Reetz, M. T., Kahakeaw, D., and Lohmer, R. (2008) Adressing the numbers problem in directed evolution. *ChemBioChem 9*, 1797−1804.
(34) Chow, M. K. M., Lomas, D. A., and Bottomley, S. P. (2004) Promiscuous beta-strand interactions and the conformational diseases. *Curr. Med. Chem. 11*, 491−499.
(35) Dooley, K., Bulutoglu, B., and Banta, S. (2014) Doubling the cross-linking interface of a rationally designed beta roll peptide for calcium-dependent proteinaceous hydrogel formation. *Biomacromolecules 15*, 3617−3624.
(36) Lesnierowski, G., and Kijowski, J. (2007) In *Bioactive Egg Compounds*, 2nd ed., pp 33−42, Springer, New York.
(37) Maroufi, B., Ranjbar, B., Khajeh, K., Naderi-Manesh, H., and Yaghoubi, H. (2008) Structural studies of hen egg-white lysozyme dimer: comparison with monomer. *Biochim. Biophys. Acta, Proteins Proteomics 1784*, 1043−1049.
(38) Burgess, R. R., and Thompson, N. E. (2002) Advances in gentle immunoaffinity chromatography. *Curr. Opin. Biotechnol. 13*, 304−308.
(39) Thompson, N. E., and Burgess, R. R. (2005) In *Analytical Separation Science*, pp 483−502, John Wiley & Sons, Hoboken, NJ.
(40) Dooley, K., Kim, Y. H., Lu, H. D., Tu, R., and Banta, S. (2012) Engineering of an environmentally responsive beta roll peptide for use as a calcium-dependent cross-linking domain for peptide hydrogel formation. *Biomacromolecules 13*, 1758−1764.
(41) Fong, B. A., and Wood, D. W. (2010) Expression and purification of ELP-intein-tagged target proteins in high cell density *E. coli* fermentation. *Microb. Cell Fact. 9*, 1−11.
(42) Binz, H. K., Amstutz, P., Kohl, A., Stumpp, M. T., Briand, C., Forrer, P., Grütter, M. G., and Plückthun, A. (2004) High-affinity binders selected from designed ankyrin repeat protein libraries. *Nat. Biotechnol. 22*, 575−582.
(43) Dreier, B., and Plückthun, A. (2012) In *Ribosome Display and Related Technologies: Methods and Protocols*, pp 261−286, Springer, New York.


DOI: 10.1021/acssynbio.7b00089
*ACS Synth. Biol.* XXXX, XXX, XXX−XXX